Equation of State for Free Energy of Homogeneous Nucleation Derived by Monte Carlo Simulations

Yuri Yamada and Yosuke Kataoka*

Department of Materials Chemistry, College of Engineering, Hosei University,
3-7-2 Kajino-cho, Koganei, Tokyo 184-8584

(Received March 20, 2002)

We performed Monte Carlo simulations for the homogeneous nucleation on supersaturated Lennard–Jones vapor phase to estimate the equation of state for free energy of the nucleation. The calculations were performed on each system with a fixed number of particles. The initial configuration was distorted cubic lattice. The sample was cooled to low temperature, where all particles become a cluster. In the second stage it was heated enough to vaporize; the monomer phase was obtained. In the third run, the stabilized cluster was heated under the condition that the cluster was not allowed to decompose. In the last run, the system was cooled from initial monomer phase with a condition that the particles were not allowed to make any connections. Helmholtz free energies of the cluster and the monomer phase were obtained by thermodynamic integration. The obtained size of critical nucleus was comparable to the results of the molecular dynamics simulation.

Model of Homogeneous Nucleation

Supersaturated vapor generates various sizes of nuclei. If the generated nucleus was smaller than a certain size, the nucleus should collapse and disappear. On the other hand, the larger nucleus should grow into a liquid droplet. The generation of the critical nucleus is the initial stage of vapor–liquid phase transition, and the size of critical nucleus and the free energy of nucleation are important factors for the growth of the liquid droplet.

The studies on the homogeneous nucleation with computer simulations have been widely performed. Yasuoka and Matsumoto carried out large-system ensemble molecular dynamics (MD) simulations and estimated the size of critical nucleus and the free energy of nucleation from the cluster size distribution.[1,2] Oh and Zeng reported cluster size dependence of the nucleation energy by constrained Monte Carlo (MC) simulations in which they applied an upper limit of the cluster size.[3] They also performed small-system grand canonical ensemble MC method in which the cluster-vapor interaction is effectively taken into account.[4] Wolde and Frenkel obtained the nucleation energy by umbrella sampling.[5] Kusaka and Oxtoby suggested an approach to cluster simulation without a cluster criterion that determines for each particle whether it belongs to cluster or vapor phase for instantaneous configuration.[6]

In this study we suggest a simple model for estimation of the nucleation energy. Figure 1 gives a summary of the model. In the upper figure, a conventional large-system model that contains large number of target particles, and according to circumstances, carrier gas particles, and the small-size nuclei have grown spontaneously in the supersaturated vapor phase. On the other hand, in the lower figure, we focus a certain number of particles N, and put N target particles without any carrier gas particles into the system. Here, two extremes are supposed for the system: namely, cluster phase and monomer phase. The former is a state in which all particles in the system are connected together as a unity cluster, and in the latter all particles are scattered. When the free energies of the cluster phase (G_{cluster}) and the one of the monomer phase (G_{monomer}) were obtained independently, their difference ΔG gave the free energy of N-particle nucleation:

$$\Delta G = G_{\mathrm{cluster}} - G_{\mathrm{monomer}}. \quad (1)$$

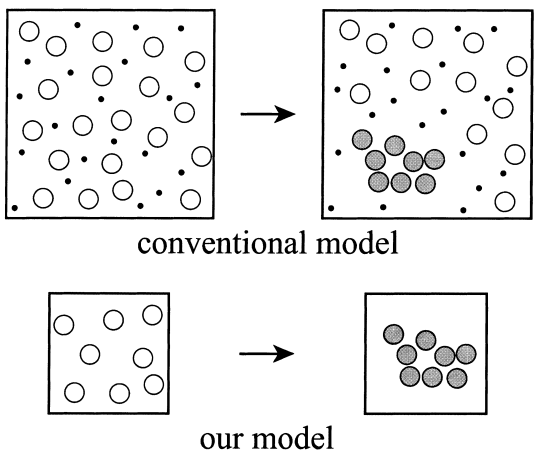

Fig. 1. The process of N-particle nucleation in the large system that includes the carrier gas particles is modeled as the nucleation of the whole particles in the N-particle system. The circles indicate the target gas particles, and the shadowed circles the nucleated particles. Though the dots indicate the carrier gas particles in the conventional model, it is not included in our model.

It is already reported that this model effectively obtains the free energy of homogeneous nucleation.[7] In this study, we estimated the equation of state for the nucleation free energy and we discuss the temperature dependence of the size of the critical nucleus and some other properties.

Monte Carlo Procedures

We used Lennard-Jones (LJ) 12-6 potential for the two-body interaction

$$u(r_{ij}) = 4\varepsilon\left\{\left(\frac{\sigma}{r_{ij}}\right)^{12} - \left(\frac{\sigma}{r_{ij}}\right)^{6}\right\}, \quad (2)$$

and the LJ parameters in reduced units: σ for length and ε for energy. Volume per particle V/N is a constant value 43.2 σ^3. This value corresponds to the one in supersaturated vapor phase and was used in recent molecular dynamics simulations by Yasuoka and Matsumoto.[1,2] Figure 2 shows the relationship between the system density and liquid-vapor coexistence curve on density-temperature plane. The curve is based on an equation of state derived by Nicolas et al.[8] The number of particles N, for which we focused respective values, is set between 2 up to 80. The basic cell that contains N target particles and no carrier gas particles is cubic, and in which we adopted periodic boundary conditions for all three dimensions. The cut-off distance of LJ interaction is a half of cell length and a correction term is adopted for contributions from more distant particles.

The detailed procedure of MC simulations is shown here. As we stated above, the cluster phase and the monomer phase should be obtained independently for the purpose of this study. Then, we performed four series of MC calculations: namely, cluster stabilization process, phase transition system, cluster phase system, and monomer phase system. The first stage, cluster stabilization, is preparation of the phase transition system and the cluster phase system. An initial configuration was chosen among distorted sc, bcc, or fcc lattice by the number of particles. If the lattice was not filled by N particles, the defect(s) was (were) inserted into the lattice site(s). Starting with the initial lattice, the particles were stabilized as a cluster by cooling MC calculation. From the initial temperature 0.20 ε/k, the system was cooled to 0.01 ε/k by 0.01 ε/k steps. We calculated at least 4 million MC steps severally for averaging and statistics at each temperature: where we regarded one MC step as N trial movements.

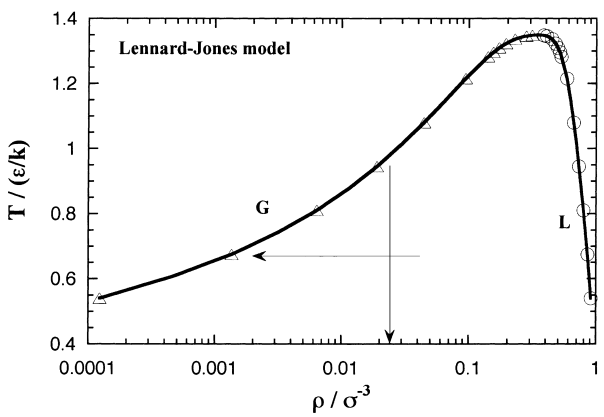

Fig. 2. Relationship between fluid-vapor coexistence curve and the system density.

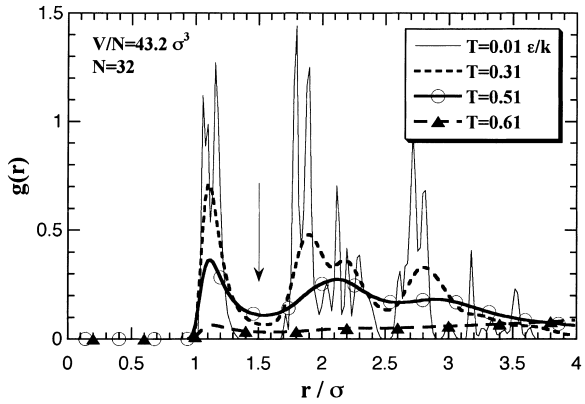

Fig. 3. Pair correlation function at several temperatures on a 32-particle system. Though the pair correlation function is usually normalized by random distribution, no normalization is performed in the figure. The peaks disappear between temperature 0.51 to 0.61 ε/k.

The second stage is phase transition system. The stabilized cluster that was created during the previous stage was heated up from 0.01 to 1.00 in 0.01 ε/k steps. One million MC steps were calculated for averaging and statistics on each temperature. The cluster decomposed to monomer phase (the supersaturated vapor) at a certain temperature. Cluster phase system, the third stage, also used the stabilized cluster as an initial configuration and was heated up similarly. However, the cluster decomposition, i.e. leaving of any particle from the cluster, is prohibited in this stage. We applied Stillinger's cluster criterion[9] for the purpose. According to Stillinger's criterion, any two particles are connected if their center-center distance is less than a threshold distance. After each MC trial, we examined the new configuration to check whether all particles of the system are mutually connected. If the new configuration was not considered as a unity cluster, it was rejected before the Metropolis judgment. The threshold distance is 1.5 σ, which has been used in several studies and corresponds to the first minimum of pair correlation function of cluster (or bulk liquid) phase, see Fig. 3. Superheated cluster phase is obtained in the third stage.

The final stage obtains monomer phase system. Contrary to the cluster phase system, any connections should be refused in this stage. That is to say, all combinations of center-center distances should be longer than 1.5 σ at every MC trials. Starting with initial temperature 1.00 ε/k, the system was cooled to 0.01 in 0.01 ε/k steps. Supercooled monomer phase is obtained in this stage. Figure 4 shows sample snapshots of the stabilized cluster, decomposed monomer phase on the phase transition system, superheated cluster phase, and supercooled monomer phase on a 32-particle system.

Free Energy Estimation

We estimated the free energy as an interaction term of Helmholtz free energy

$$A^e = U^e - TS^e, \quad (3)$$

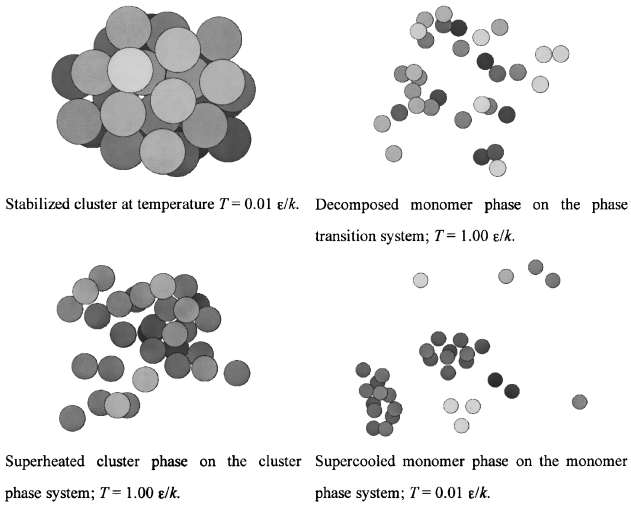

Fig. 4. Snapshots at the end of the four stages. The configurations of 32-particle system are shown as an example.

where U^e means an average value of interaction energy of the system, T temperature and S^e an interaction term of entropy. During the MC calculation, U^e can be easily obtained as the sum of two-body interaction energies as[10,11]

$$U^e = \left\langle \sum_{(ij)} u(r_{ij}) \right\rangle_{NVT}. \quad (4)$$

However, there are some difficulties in obtaining S^e. We estimated the interaction entropy as follows:[12]

$$C^e = \left(\frac{\partial U^e}{\partial T} \right)_{NV}, \text{ or} \quad (5a)$$

$$C^e = \frac{1}{kT^2} \left\{ \left\langle \left(\sum_{(ij)} u(r_{ij}) \right)^2 \right\rangle_{NVT} - \left(\left\langle \sum_{(ij)} u(r_{ij}) \right\rangle_{NVT} \right)^2 \right\}, \quad (5b)$$

$$S^e = \int_{T_0}^{T} \frac{C^e}{T} dT = \sum_i \frac{C_i^e}{T_i} \Delta T. \quad (6)$$

We adopted numerical differentiation (Eq. 5a) or the fluctuation (Eq. 5b) of the interaction energy for heat capacity estimation, and numerical integration (Eq. 6) of the heat capacity for entropy estimation. Here, in Eq. 6, each temperature interval of the numerical integration ΔT is 0.01 ε/k, and the lower end of the calculated temperature T_0 is also 0.01 ε/k, thus

$$S^e(T_0) = \frac{C^e(T_0)}{T_0} \Delta T = C^e(T_0). \quad (7)$$

Accordingly, the entropy obtained in this study is a relative value that has the same starting point as the heat capacity at $T = 0.01$ ε/k.

When the free energies of the cluster phase A^e_{cluster} and monomer phase A^e_{monomer} were obtained independently, the free energy change ΔA that accompanies with cluster formation is obtained as

$$\Delta A = A^e_{\text{cluster}} - A^e_{\text{monomer}}. \quad (8)$$

Though the ideal gas term was neglected in Eqs. 3–7, such effects were negated by subtraction in Eq. 8. Therefore, the neglect is adequate for the purpose of ΔA estimation in this study.

Monte Carlo Results

Both interaction energy and entropy increase in proportion to the number of particles in a sufficiently large system. Accordingly, we discussed about the thermodynamic quantities as values per particle.

As an example of MC results, the thermodynamic quantities of a 32-particle system are shown below. Figure 5 shows averaged interaction energy per particle versus temperature. In the phase transition system, the stabilized cluster decomposes to monomer phase at a certain temperature that depends on the number of particles. The transition temperature is ca. 0.57 ε/k in the 32-particle system. Though the equilibrated value of the decomposed monomer phase in the phase transition system should correspond to a value of the monomer phase system, they did not agree. As we stated above, each inter-particle distance was restricted to be longer than 1.5 σ in the monomer phase system, yet the restriction was not applied in the phase transition system. From this difference of condition, it is conjectured that the equilibrated interaction energy of the two systems would disagree. The monomer phase system gives an ideal monomer phase; however, we considered that the decomposed monomer phase in the phase transition system is more close to the real system. Accordingly, we corrected the curve of the monomer phase system to agree with the equilibrated value of the decomposed monomer phase in the phase transition system. Moreover, this correction aims to create a relation between the cluster phase system and the monomer phase system.

Figure 6 is the interaction term of heat capacity that is obtained from Eqs. 5a or 5b. In the figure, the results of phase transition system, cluster and monomer phase system are each shown. On the phase transition system, the temperature that indicates the maximum heat capacity corresponds to the cluster-monomer phase transition temperature 0.57 ε/k.

The interaction entropy is shown in Fig. 7. Then, the corrections for the interaction energy were also adopted for the curves of monomer phase system. In the figure, we confirmed

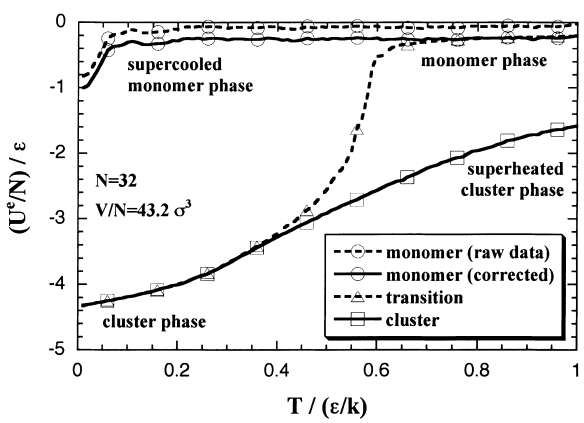

Fig. 5. Interaction energy U^e per particle versus temperature plots on 32-particle system. On the phase transition system, the cluster decomposed to monomer phase at temperature ca. 0.57 ε/k.

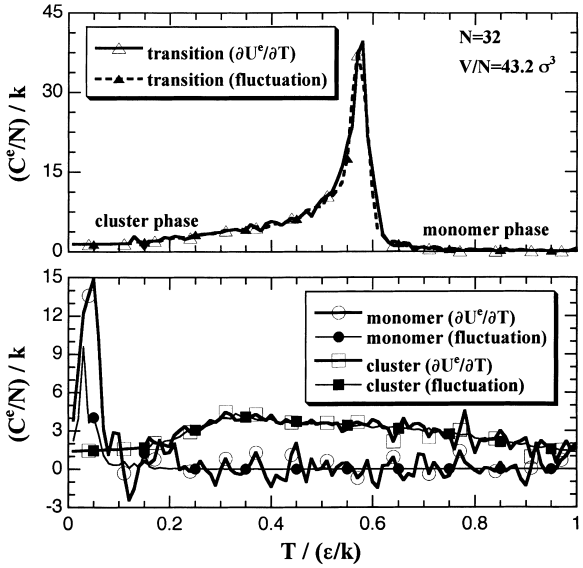

Fig. 6. Interaction term of heat capacity per particle versus temperature plots. The results of the phase transition system (the upper figure), monomer and cluster phase system (lower) are shown.

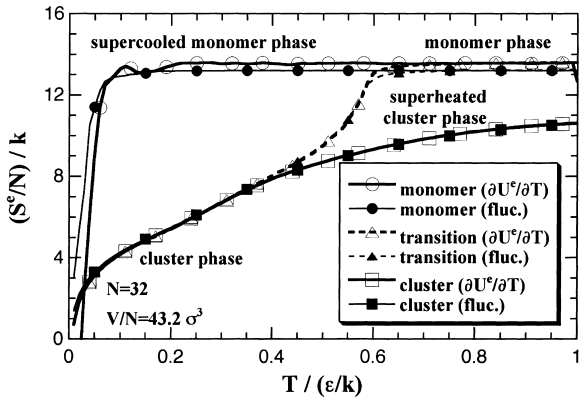

Fig. 7. Interaction entropy per particle versus temperature plots. On the three series of simulations, the curves from two ways of heat capacity calculation are nearly agreed. The curves of monomer phase are corrected to agree with the decomposed monomer phase, as similarly to the interaction energy on Fig. 5.

the equality of entropy from the two ways of the heat capacity estimation (Eqs. 5a and 5b). Accordingly, we decided to adopt the numerical differential of interaction energy for estimation of heat capacity.

The interaction term of Helmholtz free energy is shown in Fig. 8a. The intersection of the curves of cluster phase and monomer phase indicates the phase transition temperature, which is 0.55 ε/k at 32-particle system. Figure 8b is a magnification of the curves near the phase transition temperature. On the phase transition system, the cluster decomposes gradually over a certain range of temperature that is centering around the transition temperature since that configuration had no restrictions. Accordingly, a peak of the heat capacity on the phase transition system does not always agree with the intersection

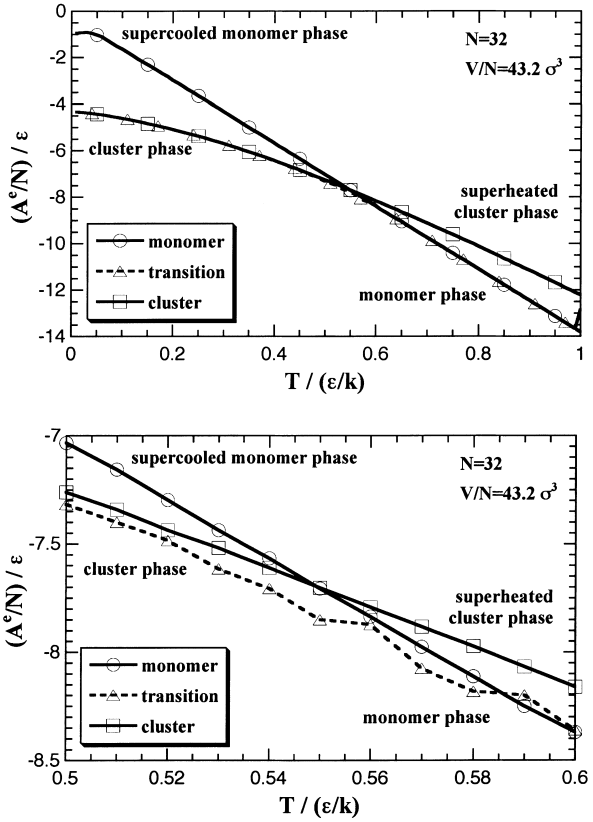

Fig. 8. (a) Interaction term of Helmholtz free energy per particle versus temperature plots on 32 particles system. The whole range of temperature is figured (the upper figure). (b) Helmholtz free energy magnified nears the phase transition temperature. The curve of monomer phase system and the cluster one have intersected at temperature 0.55 ε/k (the lower figure).

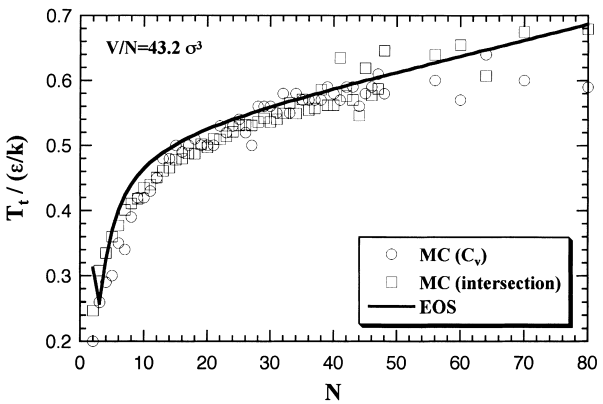

Fig. 9. Cluster-monomer phase transition temperature T_t versus number of particles plots. The circles are led from the peak of heat capacity on each numbers of particles (like Fig. 6 upper), and the squares the intersection of the curves of cluster and monomer phase system (like Fig. 8). The solid curve shows the equation of state, discussed below.

of the curves of monomer and cluster phase system. The comparison of phase transition temperature between the peak of the heat capacity and the intersection is shown in Fig. 9.

Equation of State

The interaction energy U^e, the interaction entropy S^e, the interaction term of Helmholtz free energy A^e, and the free energy change between monomer and cluster phase ΔA can be described as a function of temperature and number of particles. We designed an equation of state (EOS) for the nucleation energy ΔA as following four approximated functions:[13,14]

$$\frac{U^e_{\text{cluster}}}{NT} = \sum_m \sum_n \left\{ a_{mn} N^m \left(\frac{1}{T}\right)^n \right\}, \quad (m = -2,-1,0,1; n = -1,0,1,2,3,4,5) \tag{9a}$$

$$\frac{S^e_{\text{cluster}}}{N} = \sum_p \sum_q \{ b_{pq} N^p T^q \}, \quad (p = -2,-1,0; q = -6,-5,-4,-3,-2,-1,0,1) \tag{9b}$$

$$\frac{U^e_{\text{monomer}}}{N} = \sum_{m'} \{ a'_{m'} N^{m'} \}, \ (m' = -2,-1,0) \tag{9c}$$

$$\frac{S^e_{\text{monomer}}}{N} = \sum_{p'} \{ b'_{p'} N^{p'} \}. \ (p' = -2,-1,0) \tag{9d}$$

The functions are power series for convenience. The expression for the interaction energy of cluster phase system (Eq. 9a) is a type of high-temperature expansion for the purpose of accuracy of approximation. The expressions for monomer phase system (Eqs. 9c and 9d) depend only on the number of particles, because there is little dependence on temperature except for the two end values of the simulated temperature. The averaged values at intermediate temperature are used for such fittings.

The interaction entropy is derived from the interaction energy through the interaction heat capacity, which is followed by Eqs. 5a and 6. Accordingly, the EOS should be described by only two approximated functions, i.e. for cluster and for monomer phase system. In this study, however, we suggested four functions that treated the interaction energy U^e and the interaction entropy S^e separately. In the case of monomer phase system, we assumed that the approximated function for the interaction energy had no temperature dependence; then the heat capacity and entropy should been zero through the temperature differentiation in Eq. 5a. Accordingly, the function of the entropy should be described separately from that of the interaction energy, and we used the equilibrated values of the decomposed monomer phase in the phase transition system instead of the one of the monomer phase system. On the other hand, U^e and S^e of the cluster phase system were not approximated successfully by an equation. This may be due to the error from the limited MC step and the dispersion of MC results that is due to treating the metastable phase, superheated cluster.

The coefficients a, b, a' and b' are determined by least-squares fittings. The fitting algorithm is Modified Gram–Schmidt method.[13–15] Table 1 shows the obtained values of the coefficients.

As results of the least-squares fittings, we obtained relative deviations of the approximated functions as follows:

$$\frac{\langle [\delta(U^e_{\text{cluster}}/NT)]^2 \rangle^{1/2}}{\langle (U^e_{\text{cluster}}/NT)^2 \rangle^{1/2}} = 0.00315, \tag{10a}$$

$$\frac{\langle [\delta(S^e_{\text{cluster}}/N)]^2 \rangle^{1/2}}{\langle (S^e_{\text{cluster}}/N)^2 \rangle^{1/2}} = 0.0602, \tag{10b}$$

$$\frac{\langle [\delta(U^e_{\text{monomer}}/N)]^2 \rangle^{1/2}}{\langle (U^e_{\text{monomer}}/N)^2 \rangle^{1/2}} = 3.57 \times 10^{-4}, \tag{10c}$$

$$\frac{\langle [\delta(S^e_{\text{monomer}}/N)]^2 \rangle^{1/2}}{\langle (S^e_{\text{monomer}}/N)^2 \rangle^{1/2}} = 6.59 \times 10^{-5}. \tag{10d}$$

Figures 10–14 show the results of the least-squares fitting. The circles, triangles or squares are MC results, and the solid curve is the EOS. It can be seen that the EOS curves well re-

Table 1. Optimized Coefficients a, b, a' and b' in Eqs. 9a–9d

m	n	a_{mn}	m	n	a_{mn}	m	n	a_{mn}	m	n	a_{mn}
	−1	−2.191E−09		−1	−1.974E−07		−1	7.528E−07		−1	−5.752E−07
	0	4.542E−07		0	3.957E−05		0	−1.430E−04		0	9.862E−05
	1	−3.193E−05		1	−2.620E−03		1	8.447E−03		1	−4.404E−03
−2	2	9.597E−04	−1	2	7.106E−02	0	2	−1.750E−01	1	2	6.912E−03
	3	−3.071E−02		3	−5.011E+00		3	1.693E+01		3	−1.537E+01
	4	5.673E−02		4	4.044E+00		4	6.613E+00		4	−3.149E+01
	5	−4.054E−02		5	2.417E−01		5	−2.549E+01		5	5.267E+01

p	q	b_{pq}	p	q	b_{pq}	p	q	b_{pq}
	−6	5.841E−01		−6	−2.167E+01		−6	4.273E+01
	−5	1.581E+01		−5	−3.300E+01		−5	7.734E+00
	−4	−3.646E+00		−4	1.320E+01		−4	−1.217E+01
−2	−3	4.375E−01	−1	−3	−1.937E+00	0	−3	2.143E+00
	−2	−2.487E−02		−2	1.204E−01		−2	−1.418E−01
	−1	6.879E−04		−1	−3.488E−03		−1	4.233E−03
	0	−8.746E−06		0	4.552E−05		0	−5.612E−05
	1	3.951E−08		1	−2.087E−07		1	2.595E−07

m'	$a'_{m'}$	p'	$b'_{p'}$
−2	−2.316E−01	−2	3.761E+01
−1	4.057E−01	−1	−4.462E+01
0	−2.650E−01	0	1.547E+01

E−01 means 10^{-1}.

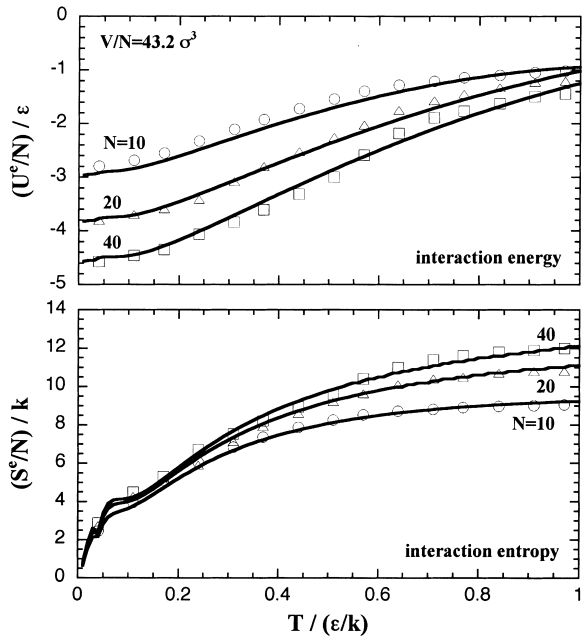

Fig. 10. Fitting results for cluster phase. Interaction energy and interaction entropy are shown versus temperature as values per particle.

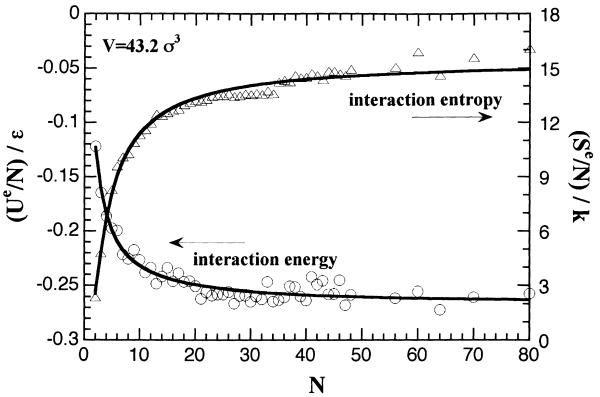

Fig. 11. Fitting results of monomer phase; U^e/N and S^e/N versus number of particles. The circles and triangles are the equilibrated values at the each numbers of particles.

produce the MC results.

As we already stated, we assumed two approximated functions for interaction energy and interaction entropy for the cluster phase system separately. Figure 14 shows the comparison between the two functions of the cluster; the interaction entropy that derived from the equation of interaction energy (Eq. 9a) by using Eqs. 5a and 6, and the expression of interaction entropy (Eq. 9b). Since the two curves agree on the whole, we confirmed the consistency of separately treating for cluster phase system with the two equations.

Figure 15 shows the critical values that were obtained by EOS. In the upper figure, the solid curve is the size of the critical nucleus and the dashed curve is the Helmholtz free energy of the critical nucleus. Both curves simply increase against the temperature. Additionally, the Helmholtz free energy is a combination of the internal energy term and the entropy term:

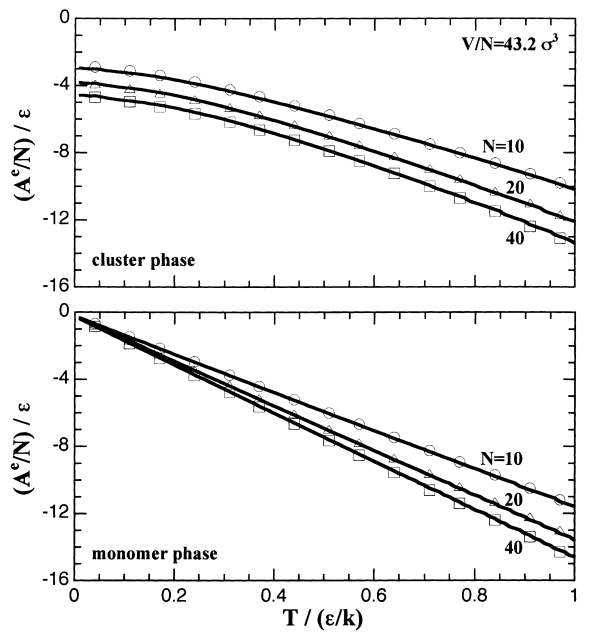

Fig. 12. Fitting results of interaction term of Helmholtz free energy per particle versus temperature. The upper figure shows the results of the cluster phase, and the lower the monomer phase.

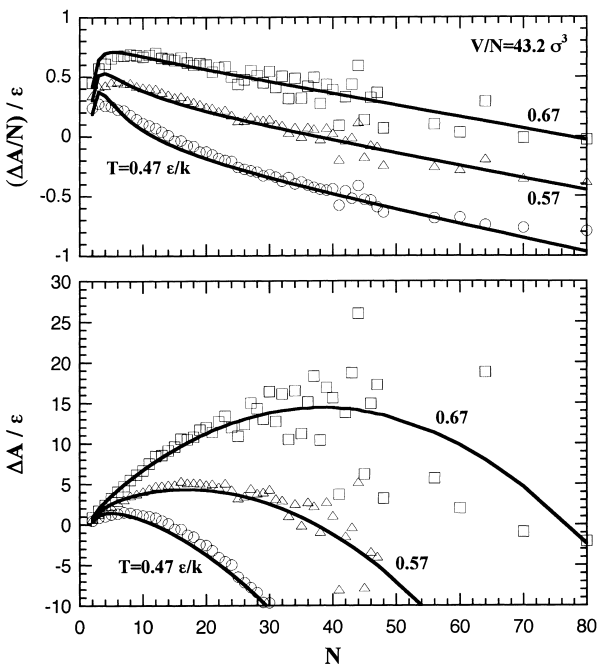

Fig. 13. Helmholtz free energy change between cluster phase and monomer phase. The upper figure shows the value per particle. The lower figure shows value of the system, a maximum is obtained about $N = 40$ at the temperature 0.67 ε/k.

$$\Delta A = \Delta U - T\Delta S, \tag{11}$$

$$\Delta U = U^e{}_{\text{cluster}} - U^e{}_{\text{monomer}}, \tag{12}$$

$$\Delta S = S^e{}_{\text{cluster}} - S^e{}_{\text{monomer}}. \tag{13}$$

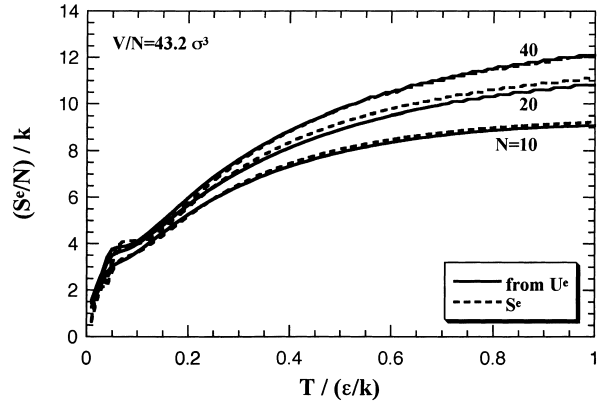

Fig. 14. Comparison between the two expressions for the cluster phase system. The solid curves show the interaction entropy that is led from the expression for the interaction energy (Eq. 9a) with Eqs. 5a and 6. The dashed curves are the expression for the interaction entropy, Eq. 9b.

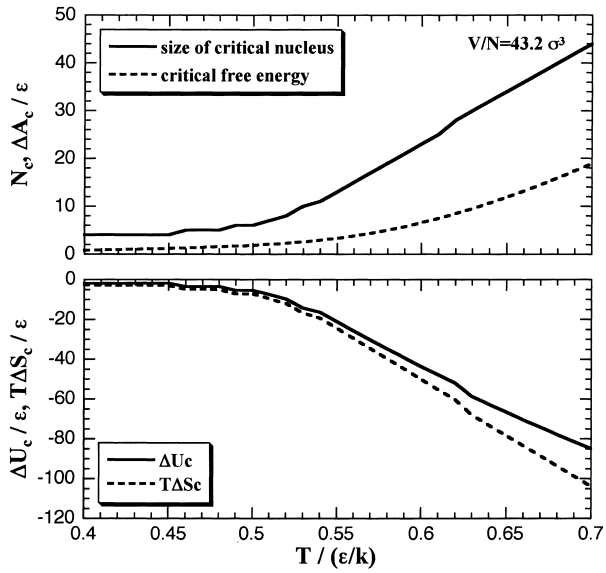

Fig. 15. Temperature dependence of the critical values of the EOS. The upper figure show the size of critical nucleus N_c and the critical free energy ΔA_c, and the lower the critical values of the internal energy term ΔU_c and the entropy term $T\Delta S_c$.

The two terms of the critical nucleus are also shown in the lower figure.

Discussion

In the usual classical theory, the free energy of homogeneous nucleation ΔG is expressed as a combination of surface term and bulk term:[1,2]

$$\Delta G = \gamma A_s + \Delta g V. \quad (14)$$

The first term is the surface term; γ is surface tension and A_s is surface area of the cluster. The second term is the bulk term; Δg is energy difference between the bulk phases and V is cluster volume. Since both A_s and V depend on the number of particles, the plot of ΔG against number of particles should have a maximum.

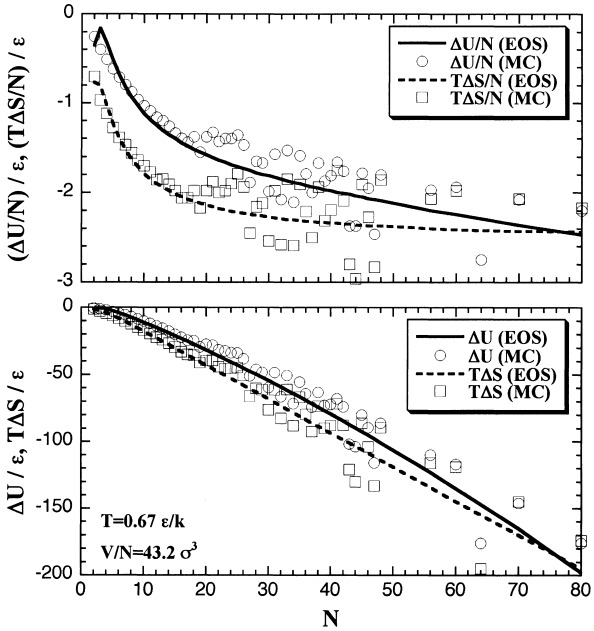

Fig. 16. Two terms of the nucleation energy versus the number of particles plots; solid curves and circles are the internal energy term ΔU, while dashed curves and squares the entropy term $T\Delta S$. Values per particle (upper) and about the system (lower) are shown.

On the other hand, in this study, the free energy of homogeneous nucleation is estimated by a combination of the internal energy term and the entropy term, like in Eqs. 11–13. The two terms ΔU and $T\Delta S$ are plotted against the number of particles in Fig. 16. As for the values per particle, both terms approach to certain values with increase of N. The internal energy term has a lower asymptotic value and approaches more slowly to the asymptote than the entropy term. Due to this behavior of the two terms, it is understood that the free energy of homogeneous nucleation has the following tendency. At the region of small number of particles, since the absolute value of the entropy term is larger than the internal energy term, ΔA gives a positive value and increases for a while. However, the entropy term is overtaken by the internal energy term with increase of N. As a result, the plot of ΔA against N has a maximum which is similarly led by the surface and bulk terms in the classical theory, and the cluster phase is more stable than the monomer phase in sufficiently large systems.

Figure 17 shows a comparison of the nucleation free energy between EOS and the classical theory at the temperature 0.67 ε/k. The EOS curve shows the size of critical nucleus and the critical nucleation energy as roughly double the values from classical theory. In comparison with the results of Yasuoka and Matsumoto,[1,2] the critical nucleation energy is overestimated (ca. 14 ε in ours and ca. 6 ε in theirs) although the size of critical nucleus is in good agreement (30–40 in theirs). However, such a direct comparison is not adequate for the following reasons. On the cluster simulations, an initial-chosen density is an overall value of the system, and the supersaturation ratio of vapor phase has decreased along with the nucleation. Yasuoka

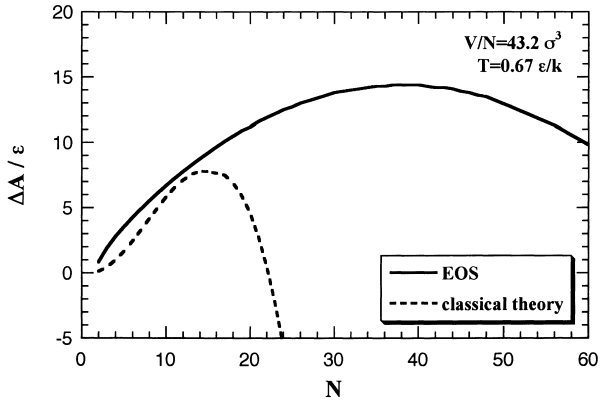

Fig. 17. Comparison on Helmholtz free energy of homogeneous nucleation between the EOS and the classical theory.

and Matsumoto re-estimated the supersaturation ratio from 14.4 to 6.8 after the nucleation.[1,2] Accordingly, the volume per particle we set in this study, 43.2 σ^3, is only available to the monomer phase. In the cluster phase system, all particles of the system belong to a cluster and the circumference of the cluster contains no particles, as if it were a vacuum. The overestimation of the size of critical nucleus and critical nucleation energy in this study is caused by the decrease of the supersaturation ratio of vapor phase.

Oh and Zeng adjusted the upper limit of the size of nucleus and the overall density of the system in their large-system simulation to control the supersaturation ratio of vapor phase.[3] In the cluster phase system of our simulations, it should be suitable to keep the vapor density at which new vapor particles are inserted into the vapor region and sampled to avoid their connection with the other vapor particles and the cluster. However, since the calculation costs considerable time, especially in the large system (in the case of $N = 64$, the run time was about one month by the fastest computers in our laboratory), some problems still remain in applications of this method.

Conclusion

We estimated free energy of homogeneous nucleation in supersaturated Lennard-Jones vapor phase with Monte Carlo simulations. Interaction term of entropy was defined by thermodynamic integration of interaction term of heat capacity, and interaction term of Helmholtz free energy was calculated with the interaction entropy and interaction energy. The free energies were separately estimated for the cluster phase and monomer phase, and the difference was obtained as the nucleation free energy. Additionally, we performed a determination of equation of state for the nucleation free energy as a function of temperature and number of particles. The determined EOS well reproduced the nucleation free energy and agreed in the size of critical nucleus with the results of recent studies.

This work is supported in part by a Grant-in Aid for Scientific Research (No. 12640504) from the Ministry of Education, Science and Culture. The authors thank the Super Computer Center, Institute for Solid State Physics. The authors thank the Research Center for Computational Science for the use of super computer. The computation was also done at Computational Science Research Center, Hosei University.

References

1 K. Yasuoka and M. Matsumoto, *J. Chem. Phys.*, **109**, 8451 (1998).
2 K. Yasuoka, Ph. D. thesis, Nagoya University (1997).
3 K. J. Oh and X. C. Zeng, *J. Chem. Phys.*, **110**, 4471 (1999).
4 K. J. Oh and X. C. Zeng, *J. Chem. Phys.*, **112**, 294 (2000).
5 P. R. ten Wolde and D. Frenkel, *J. Chem. Phys.*, **109**, 9901 (1998).
6 I. Kusaka and D. W. Oxtoby, *J. Chem. Phys.*, **110**, 5249 (1999).
7 Y. Kataoka and Y. Yamada, *Fluid Phase Equilib.*, **194–197C**, 207 (2002).
8 J. J. Nicolas, G. E. Gubbins, W. B. Streett and D. J. Tildesley, *Mol. Phys.*, **37**, 1429 (1979).
9 F. H. Stillinger, *J. Chem. Phys.*, **38**, 1486 (1963).
10 M. P. Allen and D. J. Tildesley, "Computer Simulations of Liquids," Clarendon Press, Oxford (1987).
11 R. J. Sadus, "Molecular Simulation of Fluids: Theory, Algorithms and Object-Orientation," Elsevier, Amsterdam (1999).
12 J. M. Haile, "Molecular Dynamics Simulation: Elementary Methods," Wiley Interscience, New York (1992).
13 Y. Kataoka and M. Matsumoto, *Bull. Chem. Soc. Jpn.*, **70**, 1795 (1997).
14 Y. Kataoka, *Netsu Bussei*, **13**(2), 74 (1999).
15 T. Watanabe, M. Natori and T. Oguni, "Numerical Calculation Software for Fortran77," Maruzen, Tokyo (1989).